

Generalized Compressibility in a Glass Forming Liquid

Hervé M. Carruzzo and Clare C. Yu

Department of Physics and Astronomy, University of California, Irvine, Irvine, California 92697
(February 6, 2008)

We introduce a new quantity to probe the glass transition. This quantity is a linear generalized compressibility which depends solely on the positions of the particles. We have performed a molecular dynamics simulation on a glass forming liquid consisting of a two component mixture of soft spheres in three dimensions. As the temperature is lowered, the generalized compressibility drops sharply at the glass transition. Our results are consistent with the kinetic view of the glass transition, but not with an underlying second order phase transition.

The glass transition is still not well understood despite extensive study. Experimentally the glass transition occurs when the relaxation time exceeds the measurement time and particle motion appears to be arrested. It is characterized by both kinetic and thermodynamic features. In the supercooled liquid kinetic quantities such as the viscosity and relaxation time grow rapidly as the temperature is lowered. The glass transition is also reflected in thermodynamic quantities, e.g., the specific heat at constant pressure has a step-like form and the dielectric constant has a peak at a frequency dependent temperature.

Theoretically there have been two main approaches to the problem [1,2]: dynamic and thermodynamic. The first category has been dominated by mode coupling theory (MCT) in which ideally the relaxation time diverges at a temperature T_C above the experimental glass transition [3]. The kinetic view has produced interesting and fruitful concepts such as the influence of the energy landscape on relaxation processes [4,5] and dynamic inhomogeneities [6–8]. The thermodynamic viewpoint attributes the glass transition to an underlying phase transition hidden from direct experimental observation by extremely long relaxation times [1,2,9–11]. In most scenarios there is an underlying second order phase transition associated with a growing correlation length which produces diverging relaxation times as well as diverging static susceptibilities [12–17]. More recently Mezard and Parisi [11] have argued that the underlying transition is actually a random first order transition signaled by a discontinuity in the specific heat.

In an effort to better characterize the glass transition we introduce a novel probe which we call a generalized compressibility [18]. Unlike the specific heat which monitors energy fluctuations, this linear compressibility is a function of the microscopic structure of the system: it depends solely on the positions of the particles and not on their previous history. It is a thermodynamic quantity in the sense that it is purely a function of the microstate of the system dictated by its location in phase space. It is easy to compute numerically, and it is sim-

pler than the dielectric constant which involves both the translation and orientation of electric dipoles. By performing a molecular dynamics simulation of a two component system of soft spheres, we find that the linear generalized compressibility drops sharply as the temperature decreases below the glass transition temperature T_g . The drop becomes more and more abrupt as the measurement time increases.

We now derive expressions for the linear and nonlinear generalized compressibility. To probe the density fluctuations, we follow the approach of linear response theory and consider applying an external potential $\frac{\Delta P}{\rho_o}\phi(\vec{r})$ which couples to the local density $\rho(\vec{r}) = \sum_{i=1}^N \delta(\vec{r} - \vec{r}_i)$ where \vec{r}_i denotes the position of the i^{th} particle. ρ_o is the average density. ΔP has units of pressure and sets the magnitude of the perturbation. $\phi(\vec{r})$ is a dimensionless function of position that must be compatible with the periodic boundary conditions imposed on the system, i.e., it must be continuous across the boundaries, but is otherwise arbitrary. This adds to the Hamiltonian H of the system a term

$$U = \frac{\Delta P}{\rho_o} \int_V d^3r \phi(\vec{r}) \rho(\vec{r}) = \frac{\Delta P}{\rho_o} \sum_i \phi(\vec{r}_i) \equiv \frac{\Delta P}{\rho_o} \rho_\phi \quad (1)$$

where we have defined $\rho_\phi = \int_V d^3r \phi(\vec{r}) \rho(\vec{r}) = \sum_i \phi(\vec{r}_i)$. ρ_ϕ is the inner product of ϕ and $\rho(\vec{r})$, and we can regard it as a projection of the density onto a basis function $\phi(r)$, i.e., $\rho_\phi = \langle \rho | \phi \rangle$. It weights the density fluctuations according to their spatial position. The application of the external potential will induce an average change $\delta\rho_\phi$ in ρ_ϕ :

$$\delta\rho_\phi = \langle \rho_\phi \rangle_U - \langle \rho_\phi \rangle_{U=0} \quad (2)$$

where the thermal average $\langle \rho_\phi \rangle_U$ is given by

$$\langle \rho_\phi \rangle_U = \frac{1}{\mathcal{Z}} \text{Tr} \left[e^{-\beta(H+U)} \rho_\phi \right] \quad (3)$$

The partition function $\mathcal{Z} = \text{Tr} e^{-\beta(H+U)}$ and β is the inverse temperature. For small values of ΔP , this change can be calculated using perturbation theory. Up to third order in ΔP , we find

$$\delta\rho_\phi = -\frac{\beta\Delta P}{\rho_o}\langle\rho_\phi^2\rangle_c + \frac{\beta^2\Delta P^2}{2\rho_o^2}\langle\rho_\phi^3\rangle_c - \frac{\beta^3\Delta P^3}{6\rho_o^3}\langle\rho_\phi^4\rangle_c, \quad (4)$$

where the cumulant averages are

$$\langle\rho_\phi^2\rangle_c = \langle\rho_\phi^2\rangle - \langle\rho_\phi\rangle^2 \quad (5)$$

$$\langle\rho_\phi^3\rangle_c = \langle\rho_\phi^3\rangle - 3\langle\rho_\phi\rangle\langle\rho_\phi^2\rangle + 2\langle\rho_\phi\rangle^3 \quad (6)$$

$$\langle\rho_\phi^4\rangle_c = \langle\rho_\phi^4\rangle - 4\langle\rho_\phi\rangle\langle\rho_\phi^3\rangle - 3\langle\rho_\phi^2\rangle^2 + 12\langle\rho_\phi\rangle^2\langle\rho_\phi^2\rangle - 6\langle\rho_\phi\rangle^4 \quad (7)$$

with the thermal average $\langle\rho_\phi^n\rangle = \langle\rho_\phi^n\rangle_{U=0}$. The third order cumulant, eq.(6), is zero in the liquid phase because for every configuration there exists an equivalent configuration with the opposite sign of $\rho_\phi - \langle\rho_\phi\rangle$ and so we will not consider this term any further. We can recast eq. (4) as a power series in the perturbation ΔP :

$$\frac{\delta\rho_\phi}{N} = -\frac{1}{6\rho_o k_B T}\chi_l\Delta P + \frac{1}{6(\rho_o k_B T)^3}\chi_{nl}(\Delta P)^3 \quad (8)$$

where

$$\chi_l = \frac{6}{N}\langle(\rho_\phi)^2\rangle_c \quad \chi_{nl} = -\frac{1}{N}\langle(\rho_\phi)^4\rangle_c. \quad (9)$$

where k_B is Boltzmann's constant. In the remainder of this paper we will focus our attention on the linear (χ_l) and nonlinear (χ_{nl}) dimensionless generalized compressibilities defined by the above expressions. We now discuss the choice of the function ϕ . We consider applying the potential along the direction μ of one of the coordinate axes so that $\phi(\vec{r}) = \phi(r^\mu)$. A natural candidate for $\phi(r^\mu)$ is $\cos(k_\mu r^\mu)$ with $k = 2\pi n/L$, where $n = 1, 2, \dots$ and L^3 is the volume V . In this case, ρ_ϕ is the k^{th} mode of the cosine transform of the density. However, it is sufficient to consider the simpler function $\phi(r^\mu) = |r^\mu|/L$. The absolute value means that all the particles feel a force along the μ th direction pointing towards the origin. The results are very similar to $\phi(r^\mu) = \cos(k_\mu r^\mu)$ for small k at a fraction of the computational cost. So our results in this paper correspond to $\rho_\phi = \sum_i |r_i^\mu|/L$. This is rather like a center of mass. Since the system is isotropic, we average over the direction μ .

We have performed a molecular dynamics simulation on a glass forming liquid [19,20] consisting of a 50:50 binary mixture of soft spheres in three dimensions. The two types of spheres, labelled A and B, differ only in their sizes. The interaction between two particles a distance r apart is given by $V_{\alpha\beta}(r) = \epsilon[(\sigma_{\alpha\beta}/r)^{12} + X_{\alpha\beta}(r)]$ where the interaction length $\sigma_{\alpha\beta} = (\sigma_\alpha + \sigma_\beta)/2$, $\sigma_B/\sigma_A = 1.4$ ($\alpha, \beta = A, B$). For numerical efficiency, we set the cutoff function $X_{\alpha\beta}(r) = r/\sigma_{\alpha\beta} - \lambda$ with $\lambda = 13/12^{12/13}$. The interaction is cutoff at the minimum of the potential $V_{\alpha\beta}(r)$. Energy and length are measured in units of ϵ and σ_A , respectively. Temperature is given in units

of ϵ/k_B , and time is in units of $\sigma_A\sqrt{m/\epsilon}$ where m , the mass of the particles, is set to unity. The equations of motion were integrated using the leapfrog method [21] with a time step of 0.005. During each run the temperature was kept constant using a constraint algorithm [21]. $N = N_A + N_B$ is the total number of particles. The system occupies a cube with dimensions $(\pm L/2, \pm L/2, \pm L/2)$ and periodic boundary conditions. Since N and L are fixed in any given run, the density $\rho_o = N/L^3$ is also fixed.

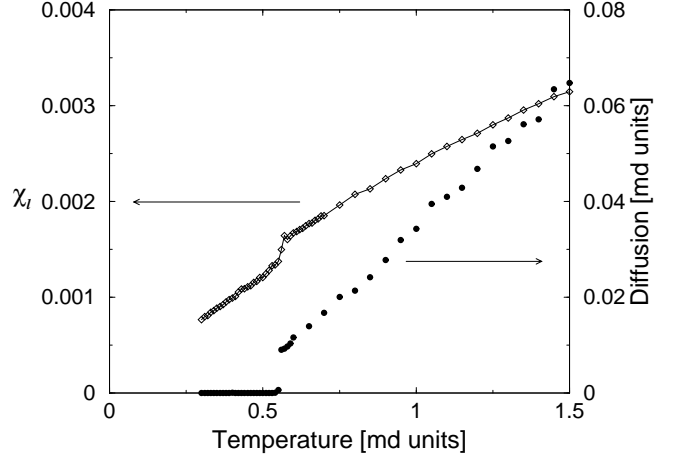


FIG. 1. Linear generalized compressibility and diffusion constant of a one component system as a function of temperature for 512 soft spheres. Crystallization is clearly seen around $T=0.57$ ($\rho_o = 1.1$). The measurement time was 10^6 md steps for each temperature. The compressibility was averaged over 5 runs while the diffusion is shown for a single run.

As a point of reference we determined the mode coupling T_C by fitting the data for the relaxation time $\tau(T)$ which is defined as the time when the self part of the intermediate scattering function $F_{s,\alpha}(\vec{k}, t)$ falls to $1/e$ [20].

$$F_{s,\alpha}(\vec{k}, t) = \frac{1}{N_\alpha} \left\langle \sum_{i=1}^{N_\alpha} e^{i\vec{k} \cdot (\vec{r}_i(t) - \vec{r}_i(0))} \right\rangle \quad (10)$$

where the subscript α refers to the particle type, A or B. We choose B particles. $\vec{r}_i(t)$ is the position of particle i at time t , and $\langle \dots \rangle$ refers to an average over different configurations. The wavevector $\vec{k} = 2\pi\vec{q}/L$ where \vec{q} is a vector of integers. For an isotropic system $F_{s,\alpha}(\vec{k}, t)$ depends only on the magnitude $k = |\vec{k}|$. We choose $k = k_{max} = 2\pi q_{max}/L$ where k_{max} is the position of the first maximum of the partial static structure factor $S(k)$. For B type particles we use $q_{max} = 8.3666$. We fit the ideal MCT form [3] $\tau(T) = A'(T - T_C)^{-\gamma}$ with $A' = 69$, $\gamma = 1.6$, $T_C = 0.306 \pm 0.005$. In finding T_C , we used data from 7 temperatures in the range $0.33 < T \leq 0.39$ below the caging temperature ($T_{cage} = 0.4$) where the intermediate scattering function first begins to show a

plateau. Our fit is consistent with the mode coupling theory requirement that $\gamma \geq 1.6$.

Our procedure for doing runs is as follows. We start each run at a high temperature ($T=1.5$) and lower the temperature in steps of $\Delta T = 0.05$. At each temperature we equilibrate for 10^4 molecular dynamics (md) steps and then measure the quantities of interest for N_τ additional steps where $N_\tau = 10^5, 2 \times 10^5, 10^6, 3 \times 10^6$ or 10^7 . All the particles move at each md step. The results are then averaged over up to 40 different initial conditions (different initial positions and velocities of the spheres).

As a check on our procedure for measuring χ_l and χ_{nl} , we consider first the case of the crystal. To this end, we consider a system of 512 identical ($\sigma_A = \sigma_B$) particles at a density $\rho_o = 1.1$. Figure 1 shows the linear compressibility and the diffusion constant as a function of temperature for the single component liquid. At high temperatures χ_l has a small slope which becomes steeper at low temperature. The salient feature is the very sharp drop around $T=0.57$ of the linear generalized compressibility and the diffusion constant. The specific heat, which is not shown, has a sharp delta function-like peak around $T=0.57$. The low temperature phase ($T < 0.57$) is a crystal with sharp Bragg peaks in the structure factor. Upon heating and cooling, the transition shows hysteresis. All these observations are consistent with the fact that crystallization is a first order transition. Not shown here is the nonlinear compressibility which is zero within our numerical error.

We now examine the response of the two component glass forming liquid. All the runs were done at a density of $\rho_o = 0.6$ and $\sigma_B/\sigma_A = 1.4$. For these parameters crystallization is avoided upon cooling.

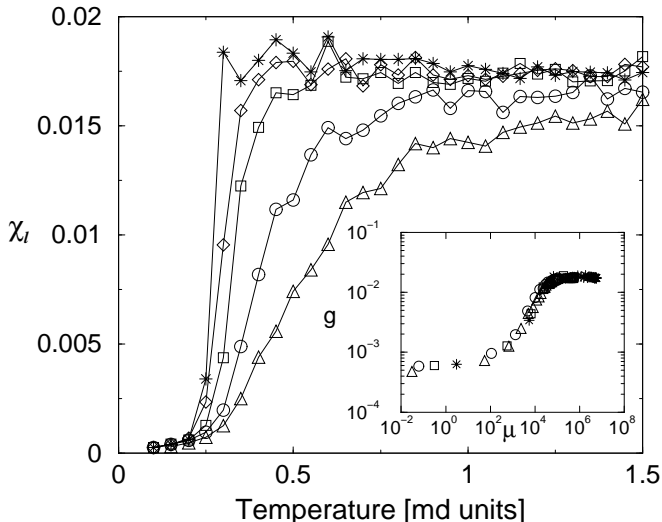


FIG. 2. Linear generalized compressibility as a function of temperature for different measuring times t_M : 10^5 (\triangle , 40 runs), 2×10^5 (\circ , 32 runs), 10^6 (\square , 10 runs), 3×10^6 (\diamond , 6 runs) and 10^7 ($*$, 4 runs) md steps. System size is 512 particles. $\rho_o = 0.6$ and $\sigma_B/\sigma_A = 1.4$. Inset: $T > T_o$ subset of the same data scaled as described in text.

Figure 2 shows the linear generalized compressibility as a function of temperature for different run times. The compressibility at high temperatures is independent of T and about an order of magnitude larger than that of the single component fluid. In the vicinity of the glass transition χ_l drops. Notice that as the measuring time t_M increases, the temperature of the drop decreases and becomes more abrupt. The linear compressibility is proportional to the width of the distribution of ρ_ϕ . If we regard ρ_ϕ as a generalized center of mass, then the drop in χ_l corresponds to the sudden narrowing of the distribution $P(\rho_\phi)$ and the sudden arrest in the fluctuations of ρ_ϕ . This behavior can be quantified using a scaling ansatz: $\chi_l(t_M, T) = g(\mu = t_M/\tau(T))$, where the characteristic time has the Vogel-Fulcher form $\tau(T) = \exp(A/(T - T_o))$. The inset of Figure 2 shows that the data collapse onto a single curve with $A = 0.75$, $T_o = 0.15$. (The data could not be fitted using $\tau(T) = \tau_{MCT}(T) = A'(T - T_C)^\gamma$ as suggested by simple mode coupling theories [3].) This value of T_o lies below the mode coupling $T_C = 0.306$, the upper bound of the glass transition temperature. Notice in Fig. 2 that the drop associated with 10^7 md steps occurs approximately at the mode coupling T_C , indicating that our long runs were in equilibrium down to the mode coupling transition temperature. This scaling suggests that χ_l becomes a step function for infinite t_M and that the drop in the compressibility would become a discontinuity at infinitely long times. This is consistent with a sudden arrest of the motion of the particles in the liquid which is the kinetic view of the glass transition. The abrupt drop also appears to be in agreement with Mezard and Parisi's proposal that the glass transition is a first order phase transition [11]. However, the drop indicates that our simulations are falling out of equilibrium and therefore we cannot really tell if there is a true thermodynamic transition.

As an independent check of the glass transition temperature, we have calculated the specific heat which is shown in Figure 3. Notice that the temperature of the peak in the specific heat agrees with the temperature at which χ_l drops.

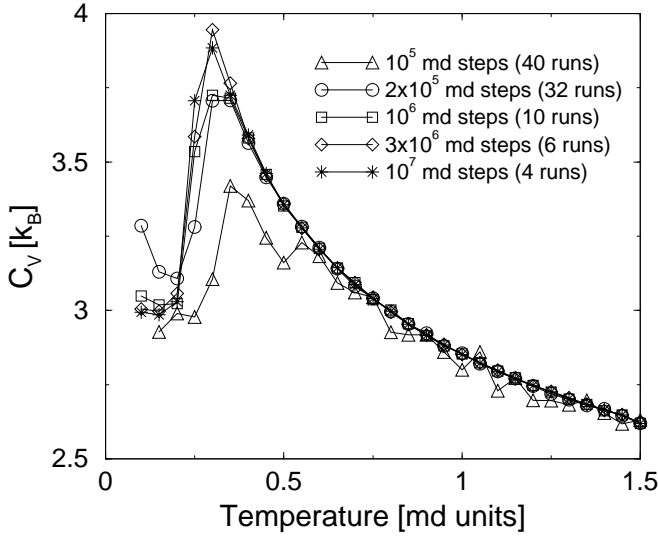


FIG. 3. Specific heat C_V at constant volume as a function of temperature calculated using energy fluctuations. All parameters are the same as in Figure 2.

The behavior seen in Figure 2 is similar to that seen in measurements of the real part of the frequency dependent dielectric function $\epsilon'(\omega)$ [17]. In that case as the frequency decreased, the temperature of the peak in $\epsilon'(\omega)$ decreased and the drop in $\epsilon'(\omega)$ below the peak became more abrupt. By extrapolating their data to $\omega = 0$, Menon and Nagel [17] argued that $\epsilon'(\omega = 0)$ should diverge at the glass transition, signaling a second order phase transition. We have looked for evidence of this divergence by examining samples of different sizes to see if the linear generalized compressibility increased systematically with system size. As shown in Figure 4 we find no size dependence and no indication of a diverging linear generalized compressibility. We also find no size dependence for the specific heat and hence, no evidence of a diverging specific heat (not shown). This is corroborated by recent MCT calculations of a molten salt which find that $\epsilon'(\omega \rightarrow 0)$ goes to a finite value as the glass transition is approached [22].

We have found hysteresis at the glass transition by first cooling a system of 512 particles to our lowest temperature $T = 0.1$ and then heating in steps of $\Delta T = 0.05$. As before we equilibrate at each temperature for 10^4 time steps and then measure quantities for an additional 10^6 time steps. Our results are shown in the inset of Figure 4. Notice the slight hysteresis with the rise in χ_l upon warming being at a slightly higher temperature than the drop in χ_l upon cooling. This hysteresis is consistent with the kinetic arrest of motion.

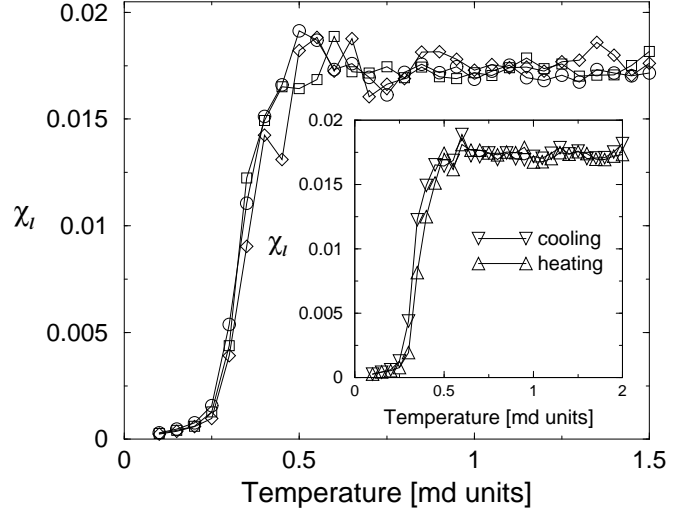


FIG. 4. Linear compressibility as a function of temperature for different system sizes: 216 (\circ , 5 runs), 512 (\square , 10 runs), and 1000 (\diamond , 5 runs) particles. The measuring time was 10^6 md steps in all cases. Inset: Linear generalized compressibility as a function of temperature for system of 512 particles upon cooling and heating. The measuring time was 10^6 md steps in both cases. The data was averaged over 10 runs. Other parameters for the main figure and the inset are the same as in Figure 2.

We now turn to the case of the nonlinear generalized compressibility χ_{nl} given by eq. (9). We are motivated by the case of spin glasses where the nonlinear magnetic compressibility diverges at the spin glass transition while the linear compressibility only has a cusp [23,24]. There have been a few studies of nonlinear response functions in real glasses [16,25], but these have not found any divergences. Our results are consistent with this conclusion. In particular we find that the nonlinear generalized compressibility is zero above and below the glass transition temperature, though it does show a glitch at the glass transition. There is no systematic increase with system size, indicating the absence of a divergence. Because χ_{nl} is sensitive to the tails of the distribution of ρ_ϕ , one must be careful to obtain a good ensemble average in the liquid above the glass transition temperature. We have done this by doing 32 runs, each involving 200,000 time steps, with different initial conditions, stringing them together as though they were one long run and then taking the appropriate averages. This produces a better ensemble average of $\langle \rho_\phi^2 \rangle^2$ which enters into χ_{nl} in eq. (6). χ_{nl} also took longer to equilibrate than χ_l . A plot χ_{nl} versus run time shows that one needs to run at least 10^6 time steps before χ_{nl} appeared to saturate.

To summarize, we have introduced a new thermodynamic quantity which depends solely on the positions of the particles and not on their histories. This quantity drops abruptly at the glass transition which is compatible with a kinetic arrest of motion, but not with an underlying second order phase transition. This generalized

compressibility can be measured experimentally. It can be directly measured in colloidal experiments which monitor the positions of the particles [26]. Measurements of the width of the distribution of ρ_q , the spatial Fourier transform of the density, would also give the linear generalized compressibility.

We thank Andrea Liu and Sharon Glotzer for helpful discussions. This work was supported in part by CULAR funds provided by the University of California for the conduct of discretionary research by Los Alamos National Laboratory.

-
- [1] M. D. Ediger, C. A. Angell, and S. R. Nagel, *J. Phys. Chem* **100**, 13200 (1996), and references therein.
 - [2] J. T. Fourkas, D. Kivelson, U. Mohanty, and K. A. Nelson, *Supercooled Liquids: Advances and Novel Applications* (American Chemical Society, Washington, D. C., 1997).
 - [3] W. Götze and L. Sjögren, *Rep. Prog. Phys.* **55**, 241 (1992).
 - [4] M. Goldstein, *J. Chem. Phys.* **51**, 3728 (1969).
 - [5] S. Sastry, P. G. Debenedetti, and F. H. Stillinger, *Nature* **393**, 554 (1998).
 - [6] C. Donati *et al.*, *Phys. Rev. Lett.* **80**, 2338 (1998).
 - [7] R. Yamamoto and A. Onuki, *J. Phys. Soc. (Japan)* **66**, 2545 (1997).
 - [8] U. Tracht *et al.*, *Phys. Rev. Lett.* **81**, 2727 (1998).
 - [9] G. Adam and J. H. Gibbs, *J. Chem. Phys.* **43**, 139 (1965).
 - [10] J. H. Gibbs and E. A. DiMarzio, *J. Chem. Phys.* **28**, 373 (1958).
 - [11] M. Mézard and G. Parisi, *Phys. Rev. Lett.* **82**, 747 (1999).
 - [12] T. R. Kirkpatrick, D. Thirumalai, and P. G. Wolynes, *Phys. Rev. A* **40**, 1045 (1989).
 - [13] J. P. Sethna, J. D. Shore, and M. Huang, *Phys. Rev. B* **44**, 4943 (1991).
 - [14] D. Kivelson *et al.*, *Physica A* **219**, 27 (1995).
 - [15] R. M. Ernst, S. R. Nagel, and G. S. Grest, *Phys. Rev. B* **43**, 8070 (1991).
 - [16] C. Dasgupta, A. V. Indrani, S. Ramaswamy, and M. K. Phani, *Europhys. Lett.* **15**, 307 (1991).
 - [17] N. Menon and S. R. Nagel, *Phys. Rev. Lett.* **74**, 1230 (1995).
 - [18] J. Yvon, *Suppl. Nuovo Cim.* **9**, 144 (1958).
 - [19] T. A. Weber and F. H. Stillinger, *Phys. Rev. B* **31**, 1954 (1985).
 - [20] W. Kob and H. C. Andersen, *Phys. Rev. Lett.* **73**, 1376 (1994).
 - [21] D. C. Rapaport, *The art of molecular dynamics simulation* (Cambridge University Press, New York, 1995).
 - [22] S. D. Wilke, H. C. Chen, and J. Bosse, *Phys. Rev. B* **60**, 3136 (1999).
 - [23] R. N. Bhatt and A. P. Young, *Phys. Rev. B* **37**, 5606 (1988).
 - [24] L. P. Levy and A. T. Ogielski, *Phys. Rev. Lett.* **57**, 3288 (1986).
 - [25] L. Wu, *Phys. Rev. B* **43**, 9906 (1991).
 - [26] E. R. Weeks *et al.*, *Science* **287**, 627 (2000).